Advances in Nano Research, *Vol. 9, No. 4 (2020) 295-307*
DOI: https://doi.org/10.12989/anr.2020.9.4.295

Vibrational characteristics of multi-phase nanocomposite reinforced circular/annular system

Changlin Zhou[1a], Yi Zhao[2], Ji Zhang[*1], Yuan Fang[2] and Mostafa Habibi[**3,4]

[1]*School of Civil and Hydraulic Engineering, Huazhong University of Science and Technology, Wuhan, Hubei, 430074, China*
[2]*China Construction Third Engineering Co., Ltd, Wuhan, Hubei, 430064, China*
[3]*Institute of Research and Development, Duy Tan University, Da Nang 550000, Vietnam*
[4]*Faculty of Electrical – Electronic Engineering, Duy Tan University, Da Nang 550000, Vietnam*

(*Received August 17, 2020, Revised October 16, 2020, Accepted October 17, 2020*)

Abstract. The vibrational characteristics of Multi-Phase Nanocomposite (MPC) reinforced annular/circular plate under initially stresses are presented using the state-space formulation based on three-dimensional elasticity theory (3D-elasticity theory) and Differential Quadrature Method (DQM). The MPC reinforced annular/circular plate is under initial lateral stress and composed of multilayers with Carbon Nanotubes (CNTs) uniformly dispersed in each layer, but its properties change layer-by-layer along the thickness direction. The State-Space based Differential Quadrature Method (SS-DQM) is presented to examine the frequency behavior of the current structure. Halpin-Tsai equations and fiber micromechanics are used in the hierarchy to predict the bulk material properties of the multi-scale composite. A singular point is investigated for modeling the circular plate. The CNTs are supposed to be randomly oriented and uniformly distributed through the matrix of epoxy resin. Afterward, a parametric study is done to present the effects of various types of sandwich circular/annular plates on frequency characteristics of the MPC reinforced annular/circular plate using 3D-elasticity theory.

Keywords: 3D-elasticity theory; SS-DQM; singular point; MPC reinforced annular/circular plate

1. Introduction

Since there are an infinite technology's demands for the mechanical properties' improvement, Multi-scale Hybrid Nanocomposite (MHN) reinforcement increases the consideration of scientists in the case of design enhancement of practical composites. The reinforcement scale highly depends on the aim of the engineer where the structure should be used. A range of composites manufactured by macroscale reinforcement including Carbon Fiber's (CFs) in a certain orientation to boost the performance of the structure mechanically (Balubaid *et al*. 2019, Berghouti *et al*. 2019, Boutaleb *et al*. 2019, Boussoula *et al*. 2020, Chikr *et al*. 2020, Ghabussi *et al*. 2020, Kaddari *et al*. 2020, Khiloun *et al*. 2020, Menasria *et al*. 2020, Rabhi *et al*. 2020, Rahmani *et al*. 2020, Refrafi *et al*. 2020, Tounsi *et al*. 2020, Zine *et al*. 2020). Recently, it is revealed that composites enriched by MHN are much more beneficial in real engineering applications (Alimirzaei *et al*. 2019, Draoui *et al*. 2019, Medani *et al*. 2019, Bourada *et al*. 2020, Bousahla *et al*. 2020).

Thereby, the dynamics of the composites enhanced by MHN is a significant area of research. Chakrapani *et al*. (2016) used a model of multiple size levels to survey the importance of fibers' and sequence of laminate directions on the CFs enriched composite beam's forced oscillation response which its viscoelasticity is determined to employ the Kelvin-Voigt equation. Furthermore, they conducted experimental research in order to confirm the numerical results' accuracy. In another investigation, buckling along with the post-buckling behavior of the fiber-reinforced beam located in a hygro-thermal environment has been scrutinized via the Reddy's model by Emam and Eltaher (2016).

On the other hand, enhancing composite properties using nano-scaled fibers instead of macro-sized ones reveals considerable boosting in the mechanics of structures. However, many scientists are focusing on the CNT-reinforced structures. For instance, a FE model is applied in order to analyze CNTR circular, and the annular plate's buckling relied on third-order SDT by Maghamikia and Jam (2011). They claimed that the load determined by their method, which is critical when it comes to the buckling investigation, is less than those calculated based on classical methods, owing to considering shear strain terms. Vibration study of continuously graded thick CNTR annular plate relying on an elastic foundation utilizing elasticity model is conducted by Tahouneh and Yas (2014). They used a solution method known as the Differential Quadrature Method (DQM) in their research paper. As another study, Tahouneh and Eskandari-Jam (2014) investigated natural frequencies of continuously graded

*Corresponding author, Ph.D.,
E-mail: zhang_ji@hust.edu.cn
**Co-corresponding author, Ph.D.,
E-mail: mostafahabibi@duytan.edu.vn
[a] Ph.D., E-mail: zclmail9919@sina.com

ISSN: 2287-237X (Print), 2287-2388 (Online)

CNTR annular plate relying on an elastic medium in which Carbon Nanotubes (CNTs) are changed through the plate's thickness, while the elasticity model and DQ method applied to obtain motion equations and solve those equations respectively. In both papers reported above, in order to estimate the composite annular plate's elastic properties, Eshelby-Mori-Tanaka micro-scaled mechanics is applied. Using variational DQM to solve the equations governed to this problem, which is extended based on the FSDT, Ansari *et al*. (2017) conducted buckling and vibration characteristics of functionally graded CNT-reinforced annular sector plate covered by an elastic foundation under thermal loading. Progress of research in the field of static, bending, and stress-strain responses of the composite structures are that Alibeigloo (2020) reported a study about the thermostatic information of a simply supported doubly curved shell that the structure is reinforced with four kinds of GPLs patterns and they formulated the problem with the aid of 3D-elasticity framework. Shaban and Alibeigloo (2020) presented a paper about the bending information of a smart panel that integrated with a piezoelectric layer. Also, they formulated the problem via elasticity theory and the energy method and solved by using the state-space method. They showed that the geometrical parameters have an important issue for studying. Rahimi *et al*. (2020) reported the static and stress-strain responses of an imperfect GPLs reinforced shell via 3D-elasticity theory, Halpin-Tsai, and Rule of mixtures. Their results show that porosity, boundary conditions, and GPLs patterns can have an important effect on the bending behavior of the inhomogeneous structure. In a comprehensive study, Safarpour *et al*. (2019a) had a focus on the static and dynamic behaviors of the GPLs reinforced imperfect circular/annular system. They derived the formulations of the problem with the aid of elasticity theory and Halpin-Tsai model. They employed a semi numerical method as a solver to draw the results of their paper. Also, Safarpour *et al*. (2019b) reported research about the static, bending, and stress-strain responses of the GPLs reinforced conical shell, cylindrical shell, and disk via elasticity theory and GDQ method. Alibeigloo and Noee (2017) presented a paper about the impact FG patterns and geometrical parameters of an inhomogeneous shell on the static and dynamic properties with the aid of 3D-elasticity theory and Fourier series analytical solution. Salehipour *et al*. (2020) had a focus on the bending and stress-strain information of the porous size-dependent FG shell via Hamilton's principle and GDQ method. Their results show that the length scale factor and imperfection factor have the most remarkable impact on the bending and frequency of the inhomogeneous shell. Parand and Alibeigloo (2017) employed 3D-elasticity theory and Kelvin-Voigt method to formulate bending and natural dynamic properties of the viscoelastic FG shell. They used Fourier series and DG method to solved the governing equation of the problem and drown their result to show the effect of viscoelastic properties on the static and dynamic behaviors of the inhomogeneous shell. Alibeigloo (2017) reported a research about the static, bending, and stress-strain information of the time dependent FG core sandwich simply supported plate under thermal shock. He employed Laplace method to solve the equation of the problem. Van Do and Lee (2020) presented a paper about the impacts of GPLs patterns on the bending, and dynamic behavior of the cylindrical and spherical panels with the aid of Halpin-Tsai model, higher-order deformation theory and isogeometric method.

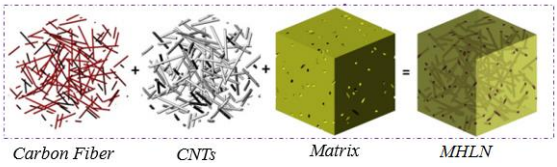

Fig. 1 Distribution patterns of CNT through the thickness of the MHLN

Also, references (Tounsi *et al*. 2013, Salari 2016, Ebrahimi and Jafari 2017, Ehyaei and Daman 2017, Wu *et al*. 2018, Ebrahimi *et al*. 2019, Ebrahimi and Salari 2019, Emdadi *et al*. 2019, Ghannadpour and Moradi 2019, Shahsavari *et al*. 2019, Dehshahri *et al*. 2020, Ebrahimi *et al*. 2020a) presented stability/instability analysis of the structures with the aid of different solution procedure.

According to the extremely detailed exploration in the literature by the authors, no one can claim there is a research on the vibration analysis of the MPCL reinforced circular/annular plates using 3D-elasticity theory. Rule of the mixture and modified Halpin-Tsai model are engaged to provide the effective material constant of the MPC disk. With the aid of compatibility conditions, the sandwich structure with two, three, five and seven layers is modeled. The SS-DQM is presented to examine the frequency behavior of Multi-scale Hybrid Laminated Nanocomposite (MHLN) Reinforced Circular/Annular Plate (MHLNRCP/ MHLNRAP) with different boundary conditions. Afterward, a parametric study is done to present the effects of stacking sequence, various types of sandwich circular/ annular plates, and various types of pressure on frequency characteristics of the MHLN reinforced circular/annular plate's 3D-elasticity theory.

2. Mathematical modeling

2.1 The homogenization process of MHLN

The procedure of homogenization is made of two main steps based upon the Halpin-Tsai model (Thostenson *et al*. 2002), together with a micromechanical theory (Shen 2009), as shown in Fig. 1. The first stage is engaged with computing the effective characteristics of the composite reinforced with CFs as following (Rafiee *et al*. 2014)

$$E_{11} = V_F E_{11}^F + V_{NCM} E^{NCM} \tag{1a}$$

$$\frac{1}{E_{22}} = \frac{V_F}{E_{22}^F} + \frac{V_{NCM}}{E^{NCM}} - V_F V_{NCM} \times \frac{\frac{(\nu^F)^2 E^{NCM}}{E_{22}^F} + \frac{(\nu^{NCM})^2 E_{22}^F}{E^M} - 2\nu^F \nu^{NCM}}{V_F E_{22}^F + V_{NCM} E^{NCM}} \tag{1b}$$

$$E_{33} = E_{22} \tag{1c}$$

$$\frac{1}{G_{12}} = \frac{V_F}{G_{12}^F} + \frac{V_{NCM}}{G^{NCM}}, \qquad G_{23} = G_{12}, \qquad G_{13} = G_{12} \tag{1d}$$

$$\rho = V_F \rho^F + V_{NCM} \rho^{NCM} \tag{1e}$$

$$\nu_{12} = V_F \nu^F + V_{NCM} \nu^{NCM} \tag{1f}$$

$$\begin{aligned} &\nu_{21} = \frac{E_{22}}{E_{11}} \nu_{12}, \qquad \nu_{13} = \nu_{12}, \qquad \nu_{31} = \nu_{21} \\ &\nu_{32} = \nu_{21}, \qquad \nu_{23} = \nu_{32} \end{aligned} \tag{1g}$$

The relation between V_F and V_{NCM} is as follows (Rafiee *et al*. 2014)

$$V_F + V_{NCM} = 1 \tag{2}$$

The second step is organized to obtain the effective characteristics of the nanocomposite matrix reinforced with CNTs with the aid of the extended Halpin-Tsai micromechanics as follows (Kim *et al*. 2009)

$$\begin{aligned} E^{NCM} = E^M \Big(&\frac{5}{8}\Big(\frac{1 + 2\beta_{dd} V_{CNT}}{1 - \beta_{dd} V_{CNT}}\Big) \\ &+ \frac{3}{8}\Big(\frac{1 + 2(l^{CNT}/d^{CNT})\beta_{dl} V_{CNT}}{1 - \beta_{dl} V_{CNT}}\Big)\Big) \end{aligned} \tag{3}$$

Here, β_{dd} and β_{dl} would be computed as the following expression

$$\begin{aligned} \beta_{dl} &= \frac{\left(\frac{E_{11}^{CNT}}{E^M}\right) - \left(\frac{d^{CNT}}{4t^{CNT}}\right)}{\left(\frac{E_{11}^{CNT}}{E^M}\right) + \left(\frac{l^{CNT}}{2t^{CNT}}\right)} \\ \beta_{dd} &= \frac{(E_{11}^{CNT}/E^M) - (d^{CNT}/4t^{CNT})}{(E_{11}^{CNT}/E^M) + (d^{CNT}/2t^{CNT})} \end{aligned} \tag{4}$$

According to the W_{CNT}, the volume fraction of CNTs can be formulated as follows (Rafiee *et al*. 2013)

$$V_{CNT}^* = \frac{W_{CNT}}{W_{CNT} + (\frac{\rho^{CNT}}{\rho^M})(1 - W_{CNT})} \tag{5}$$

Also, MHLN distribution, along with thickness direction, can be given by (Wu *et al*. 2017)

$$V_{CNT} = V_{CNT}^* \tag{6}$$

Besides, the relation between V_M and V_{CNT} is as follows

$$V_{CNT} + V_M = 1 \tag{7}$$

Finally, the mechanical properties of the nanocomposite structure can be given by

$$\rho^{NCM} = V_{CNT} \rho^{CNT} + V_M \rho^M \tag{8a}$$

$$\nu^{NCM} = \nu^M \tag{8b}$$

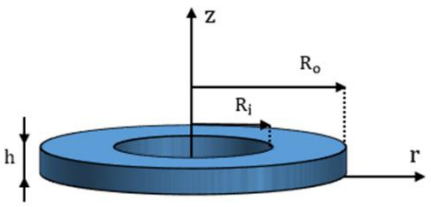

Fig. 2 Schematic view of the MPC reinforced circular plate

$$G^{NCM} = \frac{E^{NCM}}{2(1 + \nu^{NCM})} \tag{8c}$$

2.2 Obtaining governing equations

For modeling the presented structure, a cylindrical coordinate system r, θ, z located on the bottom center is employed, as shown in Fig. 2. For circular/annular plates under uniform initial stress in the circumferential direction only, its equilibrium equations in the absence of body forces are given as

$$\begin{aligned} &\frac{\partial \sigma_r}{\partial r} + \frac{1}{r}\frac{\partial \tau_{r\theta}}{\partial \theta} + \frac{\partial \tau_{rz}}{\partial z} + \frac{\sigma_r - \sigma_\theta}{r} \\ &- \frac{\sigma_0}{r^2}\left(\frac{\partial^2 u_r}{\partial \theta^2} - 2\frac{\partial u_\theta}{\partial \theta} - u_r\right) = \rho \frac{\partial^2 u_r}{\partial t^2} \end{aligned} \tag{9a}$$

$$\begin{aligned} &\frac{\partial \sigma_\theta}{r\partial \theta} + \frac{\partial \tau_{\theta z}}{\partial z} + \frac{\partial \tau_{r\theta}}{\partial r} + \frac{2\tau_{r\theta}}{r} \\ &- \frac{\sigma_0}{r^2}\left(2\frac{\partial u_r}{\partial \theta} + \frac{\partial^2 u_\theta}{\partial \theta^2} - u_\theta\right) = \rho \frac{\partial^2 u_\theta}{\partial t^2} \end{aligned} \tag{9b}$$

$$\frac{\partial \sigma_z}{\partial z} + \frac{\tau_{rz}}{r} + \frac{\partial \tau_{rz}}{\partial r} + \frac{\partial \tau_{\theta z}}{r\partial \theta} - \frac{\sigma_0}{r^2}\frac{\partial^2 u_z}{\partial \theta^2} = \rho \frac{\partial^2 u_z}{\partial t^2} \tag{9c}$$

where $\sigma_0 > 0$ indicates compressive stress and $\sigma_0 < 0$ means tensile stress for the conveniency of discussion hereafter. Stress-strain relations of multi-scale hybrid cross-ply laminated nanocomposite circular/annular plates can be written as follows (Abualnour *et al*. 2019, Belbachir *et al*. 2019, 2020, Draiche *et al*. 2019, Sahla *et al*. 2019, Allam *et al*. 2020)

$$\begin{Bmatrix} \sigma_{RR} \\ \sigma_{\theta\theta} \\ \sigma_{zz} \\ \tau_{z\theta} \\ \tau_{rz} \\ \tau_{r\theta} \end{Bmatrix} = \begin{bmatrix} \bar{Q}_{11} & \bar{Q}_{12} & \bar{Q}_{13} & 0 & 0 & 0 \\ \bar{Q}_{21} & \bar{Q}_{22} & \bar{Q}_{23} & 0 & 0 & 0 \\ \bar{Q}_{13} & \bar{Q}_{23} & \bar{Q}_{33} & 0 & 0 & 0 \\ 0 & 0 & 0 & \bar{Q}_{44} & 0 & 0 \\ 0 & 0 & 0 & 0 & \bar{Q}_{55} & 0 \\ 0 & 0 & 0 & 0 & 0 & \bar{Q}_{66} \end{bmatrix} \begin{Bmatrix} \varepsilon_{RR} \\ \varepsilon_{\theta\theta} \\ \varepsilon_{zz} \\ \gamma_{z\theta} \\ \gamma_{rz} \\ \gamma_{r\theta} \end{Bmatrix} \tag{10}$$

where (Abualnour *et al*. 2019, Draiche *et al*. 2019, Sahla *et al*. 2019, Belbachir *et al*. 2020)

$$\begin{aligned} \bar{Q}_{11} = Q_{22} \sin^4\theta + 2(Q_{12} + 2Q_{66}) \\ \sin^2\theta \cos^2\theta + Q_{11} \cos^4\theta \end{aligned} \tag{11a}$$

$$\begin{aligned} \bar{Q}_{12} = Q_{12}(\cos^4\theta + \sin^4\theta) \\ + (Q_{22} + Q_{11} - 4Q_{66}) \cos^2\theta \sin^2\theta \end{aligned} \tag{11b}$$

$$\bar{Q}_{13} = Q_{23}\,sin^2\,\theta + Q_{13}\,cos^2\,\theta \tag{11c}$$

$$\bar{Q}_{22} = Q_{11}\,sin^4\,\theta + Q_{22}\,cos^4\,\theta + 2Q_{12}\,sin^2\,\theta\,cos^2\,\theta + 2(Q_{12} + 2Q_{66})\,cos^2\,\theta\,sin^2\,\theta \tag{11d}$$

$$\bar{Q}_{23} = Q_{23}\,cos^2\,\theta + Q_{13}\,sin^2\,\theta \tag{11e}$$

$$\bar{Q}_{33} = Q_{33} \tag{11f}$$

$$\bar{Q}_{44} = Q_{55}\,sin^2\,\theta + Q_{44}\,cos^2\,\theta \tag{11g}$$

$$\bar{Q}_{55} = Q_{44}\,sin^2\,\theta - 2Q_{45}\,sin\,\theta\,cos\,\theta + Q_{55}\,cos^2\,\theta \tag{11h}$$

$$\bar{Q}_{66} = Q_{66}(cos^2\,\theta - sin^2\,\theta)^2 - 4(2Q_{12} - Q_{11} - Q_{22})\,cos^2\,\theta\,sin^2\,\theta \tag{11i}$$

The terms involved in Eq. (11) would be obtained as

$$\begin{aligned} Q_{11} &= \frac{(1 - \upsilon_{32}\upsilon_{23})}{\Delta}E_{11} \\ Q_{12} &= \frac{(\upsilon_{21} + \upsilon_{23}\upsilon_{31})}{\Delta}E_{11} \\ Q_{13} &= \frac{(\upsilon_{31} + \upsilon_{32}\upsilon_{21})}{\Delta}E_{11} \end{aligned} \tag{12a}$$

$$\begin{aligned} Q_{22} &= \frac{(1 - \upsilon_{31}\upsilon_{13})}{\Delta}E_{22} \\ Q_{23} &= \frac{(\upsilon_{32} + \upsilon_{31}\upsilon_{12})}{\Delta}E_{22} \\ Q_{33} &= \frac{(1 - \upsilon_{21}\upsilon_{12})}{\Delta}E_{33} \end{aligned} \tag{12b}$$

$$Q_{66} = G_{12}, \qquad Q_{55} = G_{13}, \qquad Q_{44} = G_{23} \tag{12c}$$

$$\Delta = (1 - \upsilon_{32}\upsilon_{23} - \upsilon_{21}\upsilon_{12} - \upsilon_{31}\upsilon_{13} - 2\upsilon_{23}\upsilon_{31}\upsilon_{12}) \tag{12d}$$

The relationships between the strain and displacement are (Safarpour *et al*. 2019a)

$$\varepsilon_r = u_{r,r}, \qquad \varepsilon_\theta = \frac{1}{r}\left(u_{\theta,\theta} + u_r\right), \qquad \varepsilon_z = u_{z,z} \tag{13a}$$

$$\begin{aligned} \gamma_{r\theta} &= \frac{1}{r}u_{r,\theta} + u_{\theta,r} - \frac{1}{r}u_\theta \\ \gamma_{rz} &= u_{r,z} + u_{z,r}, \qquad \gamma_{\theta z} = u_{\theta,z} + \frac{1}{r}u_{z,\theta} \end{aligned} \tag{13b}$$

The substitution of Eqs. (13a)-(13b) into Eq. (10) gives

$$\sigma_{rr} = \bar{Q}_{11}u_{r,r} + \frac{\bar{Q}_{12}}{r}(u_r + u_{\theta,\theta}) + \bar{Q}_{13}u_{z,z} \tag{14a}$$

$$\sigma_{\theta\theta} = \bar{Q}_{12}u_{r,r} + \frac{\bar{Q}_{22}}{r}(u_r + u_{\theta,\theta}) + \bar{Q}_{23}u_{z,z} \tag{14b}$$

$$\sigma_{zz} = \bar{Q}_{13}u_{r,r} + \frac{\bar{Q}_{23}}{r}(u_r + u_{\theta,\theta}) + \bar{Q}_{33}u_{z,z} \tag{14c}$$

$$\tau_{\theta z} = \bar{Q}_{44}\left(u_{\theta,z} + \frac{1}{r}u_{z,\theta}\right) \tag{14d}$$

$$\tau_{rz} = \bar{Q}_{55}\left(u_{r,z} + u_{z,r}\right) \tag{14e}$$

$$\tau_{r\theta} = \bar{Q}_{66}\left(\frac{1}{r}u_{r,\theta} + u_{\theta,r} - \frac{u_\theta}{r}\right) \tag{14f}$$

Employed Eqs derive State-space differential equations. Eqs. (9a)-(9c) and (14a)-(14f) as the following equations

$$\frac{\partial\sigma_z}{\partial z} = \rho\frac{\partial^2 u_z}{\partial t^2} + \frac{\sigma_0}{r^2}\frac{\partial^2 u_z}{\partial\theta^2} - \frac{\partial\tau_{rz}}{\partial r} - \frac{\tau_{rz}}{r} - \frac{1}{r}\frac{\partial\tau_{z\theta}}{\partial\theta} \tag{15a}$$

$$\frac{\partial u_r}{\partial z} = -\frac{\partial u_z}{\partial r} + \frac{\tau_{rz}}{\bar{Q}_{55}} \tag{15b}$$

$$\frac{\partial u_\theta}{\partial z} = -\frac{1}{r}\frac{\partial u_z}{\partial\theta} + \frac{\tau_{z\theta}}{\bar{Q}_{44}} \tag{15c}$$

$$\frac{\partial u_z}{\partial z} = \frac{\sigma_z}{\bar{Q}_{33}} - \frac{\bar{Q}_{13}}{\bar{Q}_{33}}\frac{\partial u_r}{\partial r} - \frac{\bar{Q}_{23}}{r\bar{Q}_{33}}u_r - \frac{\bar{Q}_{23}}{r\bar{Q}_{33}}\frac{\partial u_\theta}{\partial\theta} \tag{15d}$$

$$\begin{aligned} &\frac{\partial\tau_{rz}}{\partial z} = -\frac{\bar{Q}_{13}}{\bar{Q}_{33}}\frac{\partial\sigma_z}{\partial r} - \left(\frac{\bar{Q}_{13} - \bar{Q}_{23}}{\bar{Q}_{33}}\right)\sigma_z + \rho\frac{\partial^2 u_r}{\partial t^2} \\ &-\left(\bar{Q}_{11} - \frac{\bar{Q}_{13}^2}{\bar{Q}_{33}}\right)\frac{\partial^2 u_r}{\partial r^2} - \frac{1}{r}\left(\bar{Q}_{11} - \frac{\bar{Q}_{13}^2}{\bar{Q}_{33}}\right)\frac{\partial u_r}{\partial r} - \frac{\bar{Q}_{66}}{r^2}\times \\ &\frac{\partial^2 u_r}{\partial\theta^2} - \frac{1}{r^2}\left(\frac{\bar{Q}_{12}\bar{Q}_{33} + \bar{Q}_{23}^2 - \bar{Q}_{13}\bar{Q}_{23} - \bar{Q}_{22}\bar{Q}_{33}}{\bar{Q}_{33}}\right)u_r \\ &+\frac{\sigma_0}{r^2}\left(\frac{\partial^2 u_r}{\partial\theta^2} - 2\frac{\partial u_\theta}{\partial\theta} - u_r\right) - \frac{1}{r}(\bar{Q}_{12} + \bar{Q}_{66} - \frac{\bar{Q}_{13}\bar{Q}_{23}}{\bar{Q}_{33}}) \\ &\frac{\partial^2 u_\theta}{\partial r\partial\theta} - \frac{1}{r^2}\left(\frac{\bar{Q}_{12}\bar{Q}_{33} + \bar{Q}_{23}^2 - \bar{Q}_{13}\bar{Q}_{23} - \bar{Q}_{22}\bar{Q}_{33}}{\bar{Q}_{33}}\right)\frac{\partial u_\theta}{\partial\theta} \end{aligned} \tag{15e}$$

$$\begin{aligned} &\frac{\partial\tau_{\theta z}}{\partial z} = -\frac{1}{r}\frac{\bar{Q}_{23}}{\bar{Q}_{33}}\frac{\partial\sigma_z}{\partial\theta} - \frac{1}{r}\left(\bar{Q}_{12} + \bar{Q}_{66} - \frac{\bar{Q}_{13}\bar{Q}_{23}}{\bar{Q}_{33}}\right)\frac{\partial^2 u_r}{\partial\theta\partial r} \\ &-\frac{1}{r^2}\left(\bar{Q}_{22} + 2\bar{Q}_{66} - \frac{\bar{Q}_{23}^2}{\bar{Q}_{33}}\right)\frac{\partial u_r}{\partial\theta} - \bar{Q}_{66}\frac{\partial^2 u_\theta}{\partial^2 r} - \frac{\bar{Q}_{66}}{r}\frac{\partial u_\theta}{\partial r} \\ &-\frac{1}{r^2}\left(\bar{Q}_{22} - \frac{\bar{Q}_{23}^2}{\bar{Q}_{33}}\right)\frac{\partial^2 u_\theta}{\partial^2\theta} + \frac{2\bar{Q}_{66}}{r^2}u_\theta + \frac{\sigma_0}{r^2}\left(2\frac{\partial u_r}{\partial\theta} + \frac{\partial^2 u_\theta}{\partial\theta^2}\right. \\ &\left.-u_\theta\right) + \rho\frac{\partial^2 u_\theta}{\partial t^2} \end{aligned} \tag{15f}$$

The matrix form Eqs. (15a)-(15f) can be written

$$\frac{d\delta}{dz} = G\delta \tag{16}$$

where $\delta = \{\sigma_z u_r u_\theta u_z \tau_{rz}\tau_{\theta z}\}^T$ and G is defined in the appendix section. The relations for different boundary conditions can be formulated as follows

$$\begin{aligned} &\text{Simply:} \quad \sigma_r = u_z = u_\theta = 0 \\ &\text{Clamped:} \quad u_z = u_r = u_\theta = 0 \end{aligned} \tag{17}$$

Moreover, the singularity conditions on the central point are as follows

$$u_r = \frac{\partial u_z}{\partial r} = 0r = 0 \tag{18}$$

3. Solution procedure

Since state Eq. (16) is not possible to solve analytically, a semi-analytical procedure with the aid of the DQM technique is used to solve it. In DQM, the nth-order partial derivative of a continuous function $f(r, \theta, z)$ with respect to x at a given point r_i can be approximated to a linear sum of weighted function values at all of the discrete points as (Shu 2012)

$$\frac{\partial^n f}{\partial r^n} = \sum_{m=1}^{M} g^{(n)}{}_{j,m} f_{m,k} \tag{19}$$

Here, $g^{(n)}$ shows weighting factors for the n^{th}-order derivative in the orientation of its radius, that can be extracted as follows (Firouz and Ghadimi 2016, Gheydi *et al*. 2016, Hosseini Firouz and Ghadimi 2016, Gollou and Ghadimi 2017, Liu *et al*. 2017, Aghajani and Ghadimi 2018, Hamian *et al*. 2018, Khodaei *et al*. 2018, Leng *et al*. 2018, Akbary *et al*. 2019, Eslami *et al*. 2019, Mirzapour *et al*. 2019, Yu and Ghadimi 2019)

$$\begin{gathered} g_{ij}^{(1)} = -\sum_{j=1,\ i\neq j}^{n} g_{ij}^{(1)} \quad i = j \\ g_{ij}^{(1)} = \frac{M(x_i)}{(x_i - x_j) M(x_j)} \quad i \\ j = 1,2,\ldots,n \ \text{and} \ i \neq j \end{gathered} \tag{20}$$

where

$$M(x_i) = \prod_{j=1, j\neq i}^{n} (x_i - x_j) \tag{21}$$

The derivatives of Eq. (19) can be written as the following equations (Ghabussi *et al*. 2019, Habibi *et al*. 2019, 2020, Al-Furjan *et al*. 2020a-m, Ebrahimi *et al*. 2020b, Lori *et al*. 2020, Moayedi *et al*. 2020a, b, Oyarhossein *et al*. 2020, Safarpour *et al*. 2020, Shokrgozar *et al*. 2020)

$$\begin{gathered} g_{ii}^{(n)} = -\sum_{j=1, i\neq j}^{n} g_{ij}^{(n)} \\ 1 \le n \le N-1 \qquad \text{while} \qquad j, i = 1,2,\ldots,N \\ g_{ij}^{(n)} = r\left[g_{ij}^{(n-1)} g_{ij}^{(1)} - \frac{g_{ij}^{(n-1)}}{(x_i - x_j)} \right] \\ i \neq j \quad 2 \le n \le N-1 \quad \text{while} \quad j, i = 1,2,\ldots,N \end{gathered} \tag{22}$$

Also, using Chebyshev polynomials greed points, the seed along with the r-axes can be distributed as (Shu and Richards 1992)

$$\begin{gathered} r_i = \frac{R_0 - R_i}{2}\left(1 - cos\left(\frac{(i-1)}{(N_i - 1)}\pi\right)\right) + R_i \\ i = 1,2,3,\ldots,N_i \end{gathered} \tag{23}$$

Also, displacement fields of circular/annular plates can be given by

$$\begin{gathered} u_r = \sum_{m=1}^{\infty} \bar{u}_r \, sin(m\theta)\, e^{i\omega t} \\ u_\theta = \sum_{m=1}^{\infty} \bar{u}_\theta \, cos(m\theta)\, e^{i\omega t} \\ u_z = \sum_{m=1}^{\infty} \bar{u}_z \, sin(m\theta)\, e^{i\omega t} \end{gathered} \tag{24a}$$

$$\begin{gathered} \sigma_r = \sum_{m=1}^{\infty} \bar{\sigma}_r \, sin(m\theta)\, e^{i\omega t} \\ \sigma_\theta = \sum_{m=1}^{\infty} \bar{\sigma}_\theta \, sin(m\theta)\, e^{i\omega t} \\ \sigma_z = \sum_{m=1}^{\infty} \bar{\sigma}_z \, sin(m\theta)\, e^{i\omega t} \end{gathered} \tag{24b}$$

$$\begin{gathered} \tau_{rz} = \sum_{m=1}^{\infty} \bar{\tau}_{rz} \, sin(m\theta)\, e^{i\omega t} \\ \tau_{r\theta} = \sum_{m=1}^{\infty} \bar{\tau}_{r\theta} \, cos(m\theta)\, e^{i\omega t} \\ \tau_{\theta z} = \sum_{m=1}^{\infty} \bar{\tau}_{\theta z} \, cos(m\theta)\, e^{i\omega t} \end{gathered} \tag{24c}$$

Applying Eqs. (24a)-(24c) and (19) to Eq. (16) leads to the state equations at sampling point r_i

$$\begin{aligned} \frac{\partial \bar{\sigma}_{zi}}{\partial z} = {} & -\rho\omega^2 \bar{u}_{zi} - \frac{\sigma_0}{r_i{}^2} P_m^2 \bar{u}_{zi} \\ & - \sum_{j=1}^{N} g_{ij}\, \bar{\tau}_{rzj} - \frac{\bar{\tau}_{rzi}}{r_i} - \frac{m}{r_i} \bar{\tau}_{z\theta i} \end{aligned} \tag{25a}$$

$$\frac{\partial \bar{u}_{ri}}{\partial z} = -\sum_{j=1}^{N} g_{ij}\, \bar{u}_{zj} + \frac{\bar{\tau}_{rzi}}{\bar{Q}_{55}} \tag{25b}$$

$$\frac{\partial \bar{u}_{\theta i}}{\partial z} = -\frac{1}{r_i} m \bar{u}_{zi} + \frac{\bar{\tau}_{z\theta i}}{\bar{Q}_{44}} \tag{25c}$$

$$\begin{aligned} \frac{\partial \bar{u}_{zi}}{\partial z} = {} & \frac{\bar{\sigma}_{zi}}{\bar{Q}_{33}} - \frac{\bar{Q}_{13}}{\bar{Q}_{33}} \sum_{j=1}^{N} g_{ij}\, \bar{u}_{rj} \\ & - \frac{\bar{Q}_{23}}{r_i \bar{Q}_{33}} \bar{u}_{ri} + \frac{m\bar{Q}_{23}}{r_i \bar{Q}_{33}} \bar{u}_{\theta i} \end{aligned} \tag{25d}$$

$$\begin{aligned} \frac{\partial \bar{\tau}_{rzi}}{\partial z} = {} & -\frac{\bar{Q}_{13}}{\bar{Q}_{33}} \sum_{j=1}^{N} g_{ij}\, \bar{\sigma}_{zj} - \left(\frac{\bar{Q}_{13} - \bar{Q}_{23}}{\bar{Q}_{33}}\right) \bar{\sigma}_{zi} \\ & -\rho\omega^2 \bar{u}_{ri} - \left(\bar{Q}_{11} - \frac{\bar{Q}_{13}^2}{\bar{Q}_{33}}\right) \sum_{j=1}^{N} g_{ij}^2\, \bar{u}_{rj} \end{aligned} \tag{25e}$$

$$
\begin{aligned}
&-\frac{1}{r_i}\left(\bar{Q}_{11}-\frac{\bar{Q}_{13}^2}{\bar{Q}_{33}}\right)\sum_{j=1}^{N} g_{ij}\,\bar{u}_{rj}-\frac{1}{r_i{}^2}\\
&\left(\frac{\bar{Q}_{12}\bar{Q}_{33}+\bar{Q}_{23}^2-\bar{Q}_{13}\bar{Q}_{23}-\bar{Q}_{22}\bar{Q}_{33}}{\bar{Q}_{33}}\right)\bar{u}_{ri}\\
&+m^2\frac{\bar{Q}_{66}}{r^2}\bar{u}_{ri}-\frac{\sigma_0}{r_i{}^2}(m^2\bar{u}_{ri}-2m\bar{u}_{\theta i}+\bar{u}_{ri})
\end{aligned}
\tag{25e}
$$

$$
\begin{aligned}
&+\frac{m}{r}\left(\bar{Q}_{12}+\bar{Q}_{66}-\frac{\bar{Q}_{13}\bar{Q}_{23}}{\bar{Q}_{33}}\right)\sum_{j=1}^{N} g_{ij}\,\bar{u}_{\theta j}\\
&+\frac{m^2}{r_i{}^2}\left(\frac{\bar{Q}_{12}\bar{Q}_{33}+\bar{Q}_{23}^2-\bar{Q}_{13}\bar{Q}_{23}-\bar{Q}_{22}\bar{Q}_{33}}{\bar{Q}_{33}}\right)\bar{u}_{\theta i}
\end{aligned}
$$

$$
\begin{aligned}
&\frac{\partial\bar{\tau}_{\theta zi}}{\partial z}=-\frac{m}{r_i}\frac{\bar{Q}_{23}}{\bar{Q}_{33}}\bar{\sigma}_{zi}-\frac{m}{r_i}\left(\bar{Q}_{12}+\bar{Q}_{66}-\frac{\bar{Q}_{13}\bar{Q}_{23}}{\bar{Q}_{33}}\right)\\
&\sum_{j=1}^{N} g_{ij}\,\bar{u}_{rj}-\frac{m}{r_i{}^2}\left(\bar{Q}_{22}+2\bar{Q}_{66}-\frac{\bar{Q}_{23}^2}{\bar{Q}_{33}}\right)\bar{u}_{ri}-\bar{Q}_{66}\\
&\sum_{j=1}^{N} g_{ij}^2\,\bar{u}_{\theta j}-\frac{\bar{Q}_{66}}{r_i}\sum_{j=1}^{N} g_{ij}\,\bar{u}_{\theta j}+\frac{m^2}{r_i{}^2}\left(\bar{Q}_{22}-\frac{\bar{Q}_{23}^2}{\bar{Q}_{33}}\right)\bar{u}_{\theta i}\\
&+\frac{2\bar{Q}_{66}}{r_i{}^2}\bar{u}_{\theta i}+\frac{\sigma_0}{r_i{}^2}(2m\bar{u}_{ri}-m^2\bar{u}_{\theta i}-\bar{u}_{\theta i})-\rho\omega^2\bar{u}_{\theta i}
\end{aligned}
\tag{25f}
$$

where

$$
\begin{aligned}
&\bar{\sigma}_{ki}=\bar{\sigma}_k(r_i,\theta,z)(k=r,\theta,z)\\
&\bar{\tau}_{rzi}=\bar{\tau}_{rz}(r_i,\theta,z),\qquad \bar{\tau}_{\theta zi}=\bar{\tau}_{\theta z}(r_i,\theta,z)\\
&\bar{u}_{ki}=\bar{u}_k(r_i,\theta,z)
\end{aligned}
\tag{26}
$$

Substitution of Eqs. (17)-(18) into Eqs. (25a)-(25f) results in the following state-space equations

$$
\frac{\partial\bar{\delta}_b}{\partial\bar{z}}=\bar{G}_b\bar{\delta}_b \tag{27}
$$

in which $\bar{\delta}_b=\{\bar{\sigma}_z\ \ \bar{u}_r\ \ \bar{u}_\theta\ \ \bar{u}_z\ \ \bar{\tau}_{rz}\ \ \bar{\tau}_{\theta z}\}^T$ is the column matrix of state variables and $\bar{G}_b$ is defined in the Appendix section. Where subscript, b in Eq. (27) denotes, the state equation includes the boundary conditions. By using the layer-wise technique, $\bar{G}_b$ is reduced to the constant matrix, and then Eq. (27) can be solved analytically for N_t fictitious layer as the below

$$
\delta_k(\bar{z})=\delta_{ok}\,exp\Big(\bar{G}_{bk}(\bar{z}-\bar{z}_{k-1})\Big)\qquad \bar{z}_{k-1}\le\bar{z}\le\bar{z}_k \tag{28}
$$

where the subscript, *b*, denotes that the state equation contains the boundary conditions and the matrix $\bar{G}_b$ each boundary condition is expressed in the Appendix. Where subscript, *b* in Eq. (28) denotes, the state equation includes the boundary conditions. By using the layer-wise technique, $\bar{G}_b$ is reduced to the constant matrix, and then Eq. (28) can be solved analytically for N_t fictitious layer as the below

$$
\delta_k(\bar{z}_k)=\bar{M}_k\delta_{ok} \tag{29}
$$

in which $\bar{M}_k=exp(\frac{\bar{G}_{bk}\bar{h}_f}{N_t})$. Similarly, state-space equations can be derived by using Eq. (29).

$$
\frac{\partial\bar{\delta}_{bi}}{\partial\bar{z}}=\bar{G}_{bi}\bar{\delta}_{bi}\qquad\text{and}\qquad i=(b,b_1,b_2,m,t_2,t_1,t) \tag{30}
$$

As the repeat process, like three and five layers have

$$
\bar{\delta}_{bo}=\bar{M}_b\bar{\delta}_{bi}M_b=\prod_{k=Nt}^{1} exp\left(\frac{\bar{G}_{bk}\overline{h}_b}{N_t}\right) \tag{31a}
$$

$$
\bar{\delta}_{b_1o}=\bar{M}_{b_1}\bar{\delta}_{b_1i}M_{b1}=\prod_{k=Nt}^{1} exp\left(\frac{\bar{G}_{bk}\overline{h}_{b_1}}{N_t}\right) \tag{31b}
$$

$$
\bar{\delta}_{b_2o}=\bar{M}_{b_2}\bar{\delta}_{b_2i}M_{b2}=\prod_{k=Nt}^{1} exp\left(\frac{\bar{G}_{bk}\overline{h}_{b_2}}{N_t}\right) \tag{31c}
$$

$$
\bar{\delta}_{mo}=\bar{M}_m\bar{\delta}_{mi}M_m=\prod_{k=Nt}^{1} exp\left(\frac{\bar{G}_{bk}\overline{h}_m}{N_t}\right) \tag{31d}
$$

$$
\bar{\delta}_{t_2o}=\bar{M}_{t_2}\bar{\delta}_{t_2i}M_{t_2}=\prod_{k=Nt}^{1} exp\left(\frac{\bar{G}_{bk}\overline{h}_{t_2}}{N_t}\right) \tag{31e}
$$

$$
\bar{\delta}_{t_1o}=\bar{M}_{t_1}\bar{\delta}_{t_1i}M_{t_1}=\prod_{k=Nt}^{1} exp\left(\frac{\bar{G}_{bk}\overline{h}_{t_1}}{N_t}\right) \tag{31f}
$$

$$
\bar{\delta}_{to}=\bar{M}_t\bar{\delta}_{ti}M_t=\prod_{k=Nt}^{1} exp\left(\frac{\bar{G}_{bk}\overline{h}_t}{N_t}\right) \tag{31g}
$$

By assuming continuity of displacements and equilibrium equation at each fictitious layers, have

$$
\bar{\delta}_{to}=A\bar{\delta}_{bi} \tag{32}
$$

where $A=M_tM_{t1}M_{t2}M_mM_{b2}M_{b1}M_b$.

4. Free vibration analysis

For the free vibration behavior, the surface traction boundary condition in $\bar{z}=1/2$ and $\bar{z}=-1/2$ are as follows

$$
\begin{aligned}
&\sigma_z=\tau_{rz}=\tau_{\theta z}=0\\
&\text{at}\qquad z=-\frac{h}{2}\ \text{ and }\ \frac{h}{2}
\end{aligned}
\tag{33}
$$

Applying Eq. (33) to Eqs. (23), (26), (29) and (32) leads to the following homogenous equation.

$$
\begin{bmatrix}A_{12} & A_{13} & A_{14}\\ A_{52} & A_{53} & A_{54}\\ A_{62} & A_{63} & A_{64}\end{bmatrix}\begin{Bmatrix}\bar{u}_r\\ \bar{u}_\theta\\ \bar{u}_z\end{Bmatrix}=\begin{Bmatrix}0\\0\\0\end{Bmatrix} \tag{34}
$$

Non-trivial solution to Eq. (43) results in

Table 1 The properties of MHLNC (Karimiasl *et al*. 2019)

Carbon (fiber)	Epoxy (matrix)	Carbon nanotube
$E_{11}^{f}(GPa) = 233.05$	$v^{m} = 0.34$	$E^{cnt}\ (Gpa) = 640$
$E_{22}^{f}(GPa) = 23.1$	$\rho^{m}\ (\frac{kg}{m^3}) = 1200$	$d^{cnt}\ (m) = 0.14 \times 10^{-9}$
$G_{11}^{f}(GPa) = 8.96$	$E^{m}\ (Gpa) = 3.51$	$t^{cnt}\ (m) = 0.034 \times 10^{-9}$
$v^{f} = 0.2$		$l^{cnt}\ (m) = 0.25 \times 10^{-9}$
$\rho^{f}(\frac{kg}{m^3}) = 1750$		$\vartheta_{12} = 0.33$
		$\rho^{cnt}\ (kg/m^3) = 1350$

Table 2 Convergence number of grid points for all boundary conditions under various stacking sequence with $R_o = 1$, $R_i = 0$, $h = 0.001R_o$, $\bar{\sigma}_0 = 0$, $V_F = 0.8$, $W_{CNT} = 0.02$, circular plate, dimensionless fundamental natural frequency

Sequence layup	N = 5	N = 7	N = 9	N = 11	N = 13	N = 15	N = 17
Hinged-Simply							
$[90^0/0^0/\ldots]^7$	0.0035	0.0029	0.0030	0.0029	0.0029	0.0029	0.0029
$[0^0/90^0/\ldots]$	0.0032	0.0032	0.0033	0.0034	0.0034	0.0034	0.0034
Hinged-Clamped							
$[90^0/0^0/\ldots]^7$	0.0032	0.0032	0.0033	0.0034	0.0034	0.0034	0.0034
$[0^0/90^0/\ldots]^7$	0.0035	0.0036	0.0037	0.0037	0.0038	0.0038	0.0038

Table 3 Comparison of the first five dimensionless frequencies of an isotropic circular plate with simply boundary condition and convergence and accuracy of the DQ method is shown respect to the number of grid points. Dimensionless frequency $\omega^* = \omega r^2\sqrt{\rho h/D}$ where D is flexural rigidity $D = Eh^3/12(1-v^2)$

	ω_1^*	ω_2^*	ω_3^*	ω_4^*	ω_5^*
Azimi (1988)	4.935	29.720	74.156	-	-
Wu *et al*. (2002)	4.935	29.720	74.156	138.318	222.215
Wang *et al*. (2001)	4.9351	29.7200	74.1561	-	-
Arshid and Khorshidv (2018)	4.9371	29.7350	74.1942	138.3896	222.3303
P.S	4.4588	28.5439	72.4414	136.4673	-

$$\begin{vmatrix} A_{12} & A_{13} & A_{14} \\ A_{52} & A_{53} & A_{54} \\ A_{62} & A_{63} & A_{64} \end{vmatrix} = 0 \tag{35}$$

By solving the Eq. (35), the normalized natural frequencies of the plate can be determined. To reduce computational complexity, the frequency and initially residual stress of the MHLNRAP/MHLNRCP is non-dimensional as follows

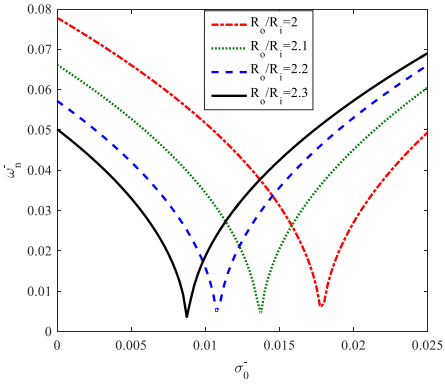

Fig. 3 Frequency of the laminated annular plate versus $\bar{\sigma}_0$ for various R_o/R_i with $h = 0.01R_i$, $R_i = 1$, $[90^0/0^0/90^0]$, $V_F = 0.8$, $W_{CNT} = 0.02$

$$\bar{\omega}_n = 100\omega_n h\sqrt{\frac{\rho_m}{E_m}}, \qquad \bar{\sigma}_0 = \frac{\sigma_0}{E_m} \tag{36}$$

5. Numerical results and discussion

Subsequently, we present a comprehensive parameter study to quantify the effects of various parameters on the bending response of MHLNRAP/MHLNRCP. The geometrical and material characteristics of constituent materials can be found in Table 1.

5.1 Convergence and validation study

Table 2 is presented to predict the convergence number of grid points for a circular plate with different boundary conditions.

According to Table 2, when the number of grid points changes from 11 to 12, we cannot see any change in the value of frequency of the circular plate, and the mentioned issue is as a fact for various boundary conditions, two kinds of layering ($[90^0/0^0/\ldots]^7$ and $[0^0/90^0/\ldots]^7$). Besides, according to Table 2, we can see two kinds of layering for the laminated structure that we called them vertical ($[90^0/0^0/\ldots]^n$) and horizontal ($[0^0/90^0/\ldots]^n$) patterns. For the circular plate with both boundary conditions, when the horizontal patterns are employed for layering, there can be the highest frequency. Furthermore, when the tension initial or residual stress in the structure increases, the natural frequency of the laminated structure decreases but for the compressive initial or residual stress, the mentioned relation is reversed.

Table 3 is presented to demonstrate the accuracy of the presented model in this paper to predict the dynamic responses of the laminated structures with mode number. According to this Table, there can be seen a good agreement between the results of our model with those in the presented work in the literature. Also, the difference between our results and the previous results is less than 2%.

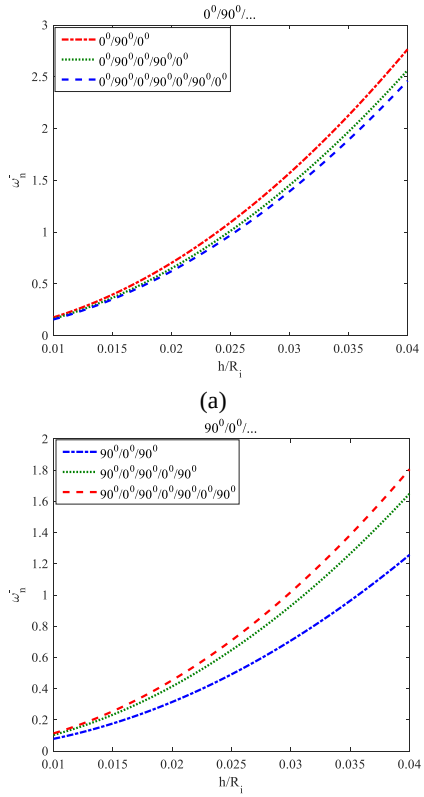

Fig. 4 Frequency of the laminated annular plate versus h/R_i for [0 90 ...] of layering in the laminated disk with R_o/R_i = 2, R_i = 1, V_F = 0.8, W_{CNT} = 0.02, $\bar{\sigma}_0$ = 0

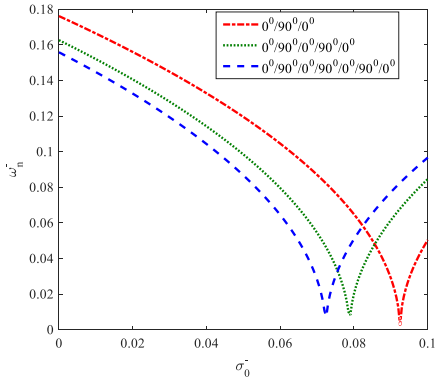

Fig. 5 Frequency of the laminated annular plate versus $\bar{\sigma}_0$ for various patterns of layering ($[90^0/0^0/\ldots]^n$ and $[0^0/90^0/\ldots]^n$) with R_o/R_i = 2, h = 0.01R_i, R_i = 1, V_F = 0.8,W_{CNT} = 0.02

5.2 Results

In this section of the presented paper, we try to report an investigation in Fig. 3 about the impacts of initial or residual stress and outer to inner radius ratio of the MPC reinforced disk (R_o/R_i) on the frequency of the structure.

From Fig. 3, it can be concluded that for each value of R_o/R_i, as the $\bar{\sigma}_0$ increases the frequency of the laminated disk reduces till critical initial stress observes.

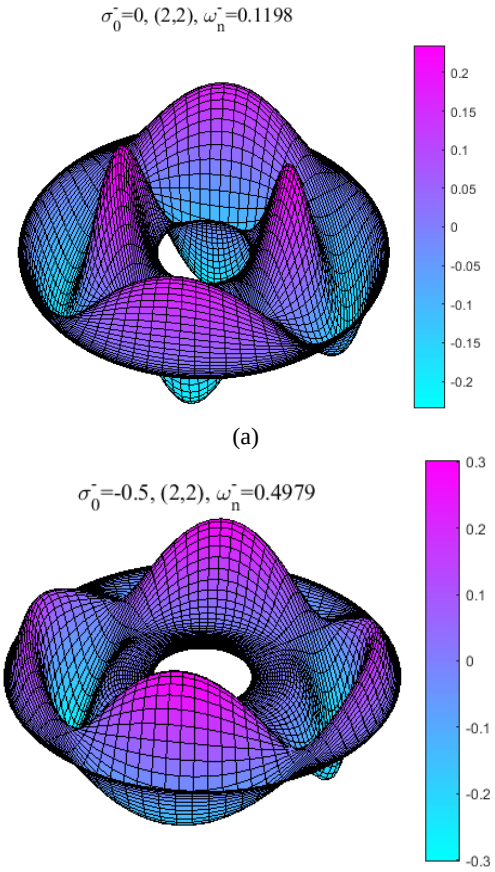

Fig. 6 Buckled mode shape of the laminated annular plate by having attention to the effect of compressive initial or residual stress with R_o/R_i = 4, h = 0.01R_i, R_i = 0.5, V_F = 0.8, W_{CNT} = 0.02, $[0^0/90^0/\ldots]^7$, Clamped-Clamped

Also, as the outer radius of the laminated disk increases, the critical initial or residual stress decreases. Fig. 4 studies the impacts of thickness to inner radius ratio (h/R_i), three kinds of boundary conditions, and various patterns of layering ($[90^0/0^0/\ldots]^n$ and $[0^0/90^0/\ldots]^n$) on the dynamics of the structure.

By having attention to Fig. 4, we can report that when the thickness of the laminated disk increases, the frequency of the structure improves, exponentially and the mentioned issue is a fact for both patterns of layering in the MPC reinforced disk. As the most impressive result, it is true that increasing the number of layers is a reason for improving the dynamic behavior of the laminated disk, but the impact of the number of the layer on the frequency is more considerable when we use the vertical patterns of layering ($[90^0/0^0/\ldots]^n$). In other words, the impact of increasing the number of layers on the frequency of the disk hardly depends on the patterns of layering, and the mentioned impact is more remarkable, when the pattern of layering is $[90^0/0^0/\ldots]^n$.

We try to report an investigation in Fig. 5 about the impacts of initial or residual stress, the number of layers in the laminated disk, and various patterns of layering ($[90^0/0^0/\ldots]^n$ and $[0^0/90^0/\ldots]^n$) on the frequency of the

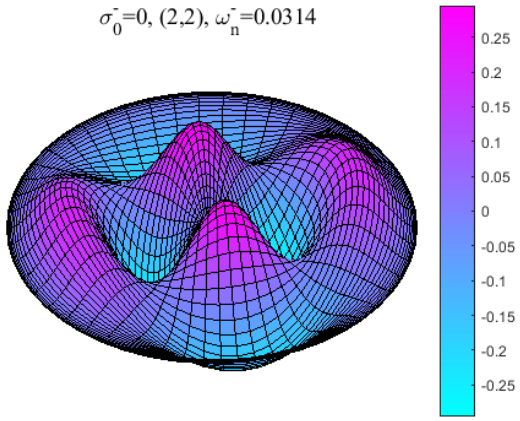

(a)

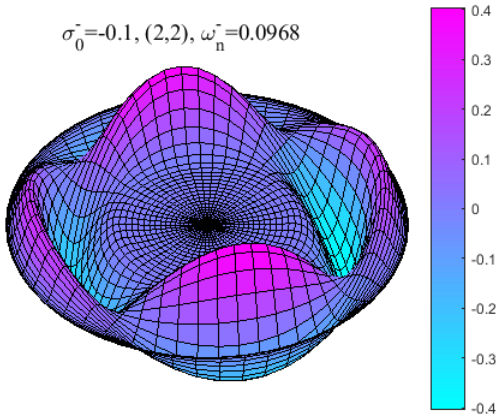

(b)

Fig. 7 Different buckled mode shape of the laminated circular plate by having attention to the effect of compressive initial or residual stress with R_o = 1, h = 0.001R_0, R_i = 0, V_F = 0.8, $[0^0/90^0/\ldots]^7$ and Hinged-Clamped

current structure.

From Fig. 5 it can be concluded that for each boundary conditions and vertical patterns of layering ($[90^0/0^0/\ldots]^n$), when the number of the layer increases, the critical initial or residual stress increases but for horizontal patterns of layering ($[0^0/90^0/\ldots]^n$), with each increase in the number of layers the critical value of $\bar{\sigma}_0$ decreases. in other words, the impact of the number of layers on the critical residual stress hardly depends on the patterns of layering, and the mentioned impact has a direct and indirect effect when the patterns of layering are $[90^0/0^0/\ldots]^n$ and $[0^0/90^0/\ldots]^n$, respectively.

In Fig. 6, different buckled mode shape of the MPC reinforced annular plate is presented with clamped-clamped boundary conditions and by having attention to the effect of compressive initial or residual stress. If we pay attention to Fig. 6, we can find that as the initial stress increases, the maximum deflection in the laminated disk increases. Also, with more exactitude, it can be concluded that when the value of initial stress increases, the concentration of deformation in the composite disk reduces along the radial direction and intensifies along the circumferential direction.

The mode shape of the MPC reinforced circular plate is presented in Fig. 7 with clamped boundary conditions and by having attention to the effect of compressive initial or residual stress. If we pay attention to Fig. 7, we can find that as the initial stress increases, the maximum deflection in the MPC reinforced circular plate increases. When the value of initial stress increases, the deformation in the composite circular plate occurs at the outer radius of the annular plate. In other words, as the initial stress increases, the concentration of deformation in the composite circular plate intensifies along the circumferential direction.

6. Conclusions

Three-elasticity approach for frequency and mode shape information of the MPC reinforced annular/circular plate under initially stress for various sets of boundary conditions were presented. The SS-DQM is presented to examine the frequency behavior of MPC reinforced annular/circular plate. Rule of the mixture and modified Halpin-Tsai model are engaged to provide the effective material constant of the presented structure. Finally, the most bolded results of this paper are as follows:

• When the tension initial or residual stress in the structure increases, the natural frequency of the MPC reinforced annular/circular plate decreases, but for the compressive initial or residual stress, the mentioned relation is reversed.

• For each value of R_o/R_i, as the $\bar{\sigma}_0$ increases the frequency of the MPC reinforced annular/circular plate reduces till critical initial stress observes.

• The impact of increasing the number of layers on the frequency of the MPC reinforced annular/circular plate is hardly depending on the patterns of layering, and the mentioned impact is more remarkable when the pattern of layering is $[900/00/\ldots]^n$.

• As the initial stress increases, the maximum deflection in the MPC reinforced annular/circular plate increases, and this issue is more remarkable in the higher mode numbers.

Acknowledgments

Financial support by the National Natural Science Foundation of China (NSFC) (Grant Nos. 51378377, 41872001), Fundamental Research Funds for the Central Universities (Grant No. 2016YXMS094), and China Construction Third Engineering Bureau Group Co., Ltd (grant No. CSCEC3Z-2019-03) is much appreciated.

References

Abualnour, M., Chikh, A., Hebali, H., Kaci, A., Tounsi, A., Bousahla, A.A. and Tounsi, A. (2019), "Thermomechanical analysis of antisymmetric laminated reinforced composite plates using a new four variable trigonometric refined plate theory", *Comput. Concrete, Int. J.*, **24**(6), 489-498. https://doi.org/10.12989/cac.2019.24.6.489.

Aghajani, G. and Ghadimi, N. (2018), "Multi-objective energy management in a micro-grid", *Energy Rep.*, **4**, 218-225.

https://doi.org/10.1016/j.egyr.2017.10.002.
Akbary, P., Ghiasi, M., Pourkheranjani, M.R.R., Alipour, H. and Ghadimi, N. (2019), "Extracting appropriate nodal marginal prices for all types of committed reserve", *Comput. Econ.*, **53**(1), 1-26. https://doi.org/10.1007/s10614-017-9716-2.
Al-Furjan, M., Alzahrani, B., Shan, L., Habibi, M. and Jung, D.W. (2020a), "Nonlinear forced vibrations of nanocomposite-reinforced viscoelastic thick annular system under hygrothermal environment", *Mech. Based Des. Struct. Mach.*, **2020**, 1-27. https://doi.org/10.1080/15397734.2020.1824795.
Al-Furjan, M., Bolandi, S.Y., Shan, L., Habibi, M. and Jung, D.W. (2020b), "On the vibrations of a high-speed rotating multi-hybrid nanocomposite reinforced cantilevered microdisk", *Mech. Based Des. Struct. Mach.*, **2020**, 1-29. https://doi.org/10.1080/15397734.2020.1828098.
Al-Furjan, M., Fereidouni, M., Habibi, M., Abd Ali, R., Ni, J. and Safarpour, M. (2020c), "Influence of in-plane loading on the vibrations of the fully symmetric mechanical systems via dynamic simulation and generalized differential quadrature framework", *Eng. Comput.*, **2020**, 1-23. https://doi.org/10.1007/s00366-020-01177-7.
Al-Furjan, M., Habibi, M. and Safarpour, H. (2020d), "Vibration control of a smart shell reinforced by graphene nanoplatelets", *Int. J. Appl. Mech.*, **12**(6), 2050066. https://doi.org/10.1142/S1758825120500660.
Al-Furjan, M., Habibi, M., Chen, G., Safarpour, H., Safarpour, M. and Tounsi, A. (2020e), "Chaotic oscillation of a multi-scale hybrid nano-composites reinforced disk under harmonic excitation via GDQM", *Compos. Struct.*, **252**, 112737. https://doi.org/10.1016/j.compstruct.2020.112737.
Al-Furjan, M., Habibi, M., Chen, G., Safarpour, H., Safarpour, M. and Tounsi, A. (2020f), "Chaotic simulation of the multi-phase reinforced thermo-elastic disk using GDQM", *Eng. Comput.*, **2020**, 1-24. https://doi.org/10.1007/s00366-020-01144-2.
Al-Furjan, M., Habibi, M., Jung, D.W, Sadeghi, S., Safarpour, H., Tounsi, A. and Chen, G. (2020g), "A computational framework for propagated waves in a sandwich doubly curved nanocomposite panel", *Eng. Comput.*, **2020**, 1-18. https://doi.org/10.1007/s00366-020-01130-8.
Al-Furjan, M., Habibi, M., Jung, D.W., Chen, G., Safarpour, M. and Safarpour, H. (2020h), "Chaotic responses and nonlinear dynamics of the graphene nanoplatelets reinforced doubly-curved panel", *Eur. J. Mech. A Solids*, **85**, 104091. https://doi.org/10.1016/j.euromechsol.2020.104091.
Al-Furjan, M., Mohammadgholiha, M., Alarifi, I.M., Habibi, M. and Safarpour, H. (2020i), "On the phase velocity simulation of the multi curved viscoelastic system via an exact solution framework", *Eng. Comput.*, **2020**, 1-17. https://doi.org/10.1007/s00366-020-01152-2.
Al-Furjan, M., Oyarhossein, M.A., Habibi, M., Safarpour, H. and Jung, D.W. (2020j), "Frequency and critical angular velocity characteristics of rotary laminated cantilever microdisk via two-dimensional analysis", *Thin-Wall. Struct.*, **157**, 107111. https://doi.org/10.1016/j.tws.2020.107111.
Al-Furjan, M., Oyarhossein, M.A., Habibi, M., Safarpour, H. and Jung, D.W. (2020k), "Wave propagation simulation in an electrically open shell reinforced with multi-phase nanocomposites", *Eng. Comput.*, **2020**, 1-17. https://doi.org/10.1007/s00366-020-01167-9.
Al-Furjan, M., Oyarhossein, M.A., Habibi, M., Safarpour, H., Jung, D.W. and Tounsi, A. (2020l), "On the wave propagation of the multi-scale hybrid nanocomposite doubly curved viscoelastic panel", *Compos. Struct.*, **255**, 112947. https://doi.org/10.1016/j.compstruct.2020.112947
Al-Furjan, M., Safarpour, H., Habibi, M., Safarpour, M. and Tounsi, A. (2020m), "A comprehensive computational approach for nonlinear thermal instability of the electrically FG-GPLRC disk based on GDQ method", *Eng. Comput.*, **2020**, 1-18. https://doi.org/10.1007/s00366-020-01088-7.
Alibeigloo, A. (2017), "Three dimensional coupled thermoelasticity solution of sandwich plate with FGM core under thermal shock", *Compos. Struct.*, **177**, 96-103. https://doi.org/10.1016/j.compstruct.2017.06.046.
Alibeigloo, A. (2020), "Three-dimensional thermoelasticity analysis of graphene platelets reinforced cylindrical panel", *Eur. J. Mech. A Solids*, **81**, 103941. https://doi.org/10.1016/j.euromechsol.2019.103941.
Alibeigloo, A. and Noee, A.R.P. (2017), "Static and free vibration analysis of sandwich cylindrical shell based on theory of elasticity and using DQM", *Acta Mechanica*, **228**(12), 4123-4140. https://doi.org/10.1007/s00707-017-1914-4.
Alimirzaei, S., Mohammadimehr, M. and Tounsi, A. (2019), "Nonlinear analysis of viscoelastic micro-composite beam with geometrical imperfection using FEM: MSGT electro-magneto-elastic bending, buckling and vibration solutions", *Struct. Eng. Mech., Int. J.*, **71**(5), 485-502. https://doi.org/10.12989/sem.2019.71.5.485.
Allam, O., Draiche, K., Bousahla, A.A., Bourada, F., Tounsi, A., Benrahou, K.H., Mahmoud, S., Adda Bedia, E. and Tounsi, A. (2020), "A generalized 4-unknown refined theory for bending and free vibration analysis of laminated composite and sandwich plates and shells", *Comput. Concrete, Int. J.*, **26**(2), 185-201. http://dx.doi.org/10.12989/cac.2020.26.2.185.
Ansari, R., Torabi, J. and Shojaei, M.F. (2017), "Buckling and vibration analysis of embedded functionally graded carbon nanotube-reinforced composite annular sector plates under thermal loading", *Compos. Part B Eng.*, **109**, 197-213. https://doi.org/10.1016/j.compositesb.2016.10.050.
Arshid, E. and Khorshidvand, A.R. (2018), "Free vibration analysis of saturated porous FG circular plates integrated with piezoelectric actuators via differential quadrature method", *Thin-Wall. Struct.*, **125**, 220-233. https://doi.org/10.1016/j.tws.2018.01.007.
Azimi, S. (1988), "Free vibration of circular plates with elastic edge supports using the receptance method", *J. Sound Vib.*, **120**(1), 19-35. https://doi.org/10.1016/0022-460X(88)90332-X.
Balubaid, M., Tounsi, A., Dakhel, B. and Mahmoud, S. (2019), "Free vibration investigation of FG nanoscale plate using nonlocal two variables integral refined plate theory", *Comput. Concrete, Int. J.*, **24**(6), 579-586. https://doi.org/10.12989/cac.2019.24.6.579.
Belbachir, N., Draich, K., Bousahla, A.A., Bourada, M., Tounsi, A. and Mohammadimehr, M. (2019), "Bending analysis of anti-symmetric cross-ply laminated plates under nonlinear thermal and mechanical loadings", *Steel Compos. Struct., Int. J.*, **33**(1), 81-92. https://doi.org/10.12989/scs.2019.33.1.081.
Belbachir, N., Bourada, M., Draiche, K., Tounsi, A., Bourada, F., Bousahla, A.A. and Mahmoud, S. (2020), "Thermal flexural analysis of anti-symmetric cross-ply laminated plates using a four variable refined theory", *Smart Struct. Syst., Int. J.*, **25**(4), 409-422. https://doi.org/10.12989/sss.2020.25.4.409.
Berghouti, H., Adda Bedia, E., Benkhedda, A. and Tounsi, A. (2019), "Vibration analysis of nonlocal porous nanobeams made of functionally graded material", *Adv. Nano Res., Int. J.*, **7**(5), 351-364. https://doi.org/10.12989/anr.2019.7.5.351.
Bourada, F., Bousahla, A.A., Tounsi, A., Bedia, E., Mahmoud, S., Benrahou, K.H. and Tounsi, A. (2020), "Stability and dynamic analyses of SW-CNT reinforced concrete beam resting on elastic-foundation", *Comput. Concrete, Int. J.*, **25**(6), 485-495. https://doi.org/10.12989/cac.2020.25.6.485
Bousahla, A.A., Bourada, F., Mahmoud, S., Tounsi, A., Algarni, A., Bedia, E. and Tounsi, A. (2020), "Buckling and dynamic behavior of the simply supported CNT-RC beams using an integral-first shear deformation theory", *Comput. Concrete, Int.*

J., **25**(2), 155-166. https://doi.org/10.12989/cac.2020.25.2.155.

Boussoula, A., Boucham, B., Bourada, M., Bourada, F., Tounsi, A., Bousahla, A.A. and Tounsi, A. (2020), "A simple nth-order shear deformation theory for thermomechanical bending analysis of different configurations of FG sandwich plates", *Smart Struct. Syst., Int. J.*, **25**(2), 197-218. https://doi.org/10.12989/sss.2020.25.2.197.

Boutaleb, S., Benrahou, K.H., Bakora, A., Algarni, A., Bousahla, A.A., Tounsi, A., Tounsi, A. and Mahmoud, S. (2019), "Dynamic analysis of nanosize FG rectangular plates based on simple nonlocal quasi 3D HSDT", *Adv. Nano Res., Int. J.*, **7**(3), 191-208. https://doi.org/10.12989/anr.2019.7.3.191.

Chakrapani, S.K., Barnard, D.J. and Dayal, V. (2016), "Nonlinear forced vibration of carbon fiber/epoxy prepreg composite beams: Theory and experiment", *Compos. Part B Eng.*, **91**, 513-521. https://doi.org/10.1016/j.compositesb.2016.02.009.

Chikr, S.C., Kaci, A., Bousahla, A.A., Bourada, F., Tounsi, A., Bedia, E., Mahmoud, S., Benrahou, K.H. and Tounsi, A. (2020), "A novel four-unknown integral model for buckling response of FG sandwich plates resting on elastic foundations under various boundary conditions using Galerkin's approach", *Geomech. Eng., Int. J.*, **21**(5), 471-487. https://doi.org/10.12989/gae.2020.21.5.471.

Dehshahri, K., Nejad, M.Z., Ziaee, S., Niknejad, A. and Hadi, A. (2020), "Free vibrations analysis of arbitrary three-dimensionally FGM nanoplates", *Adv. Nano Res., Int. J.*, **8**(2), 115-134. https://doi.org/10.12989/anr.2020.8.2.115.

Draiche, K., Bousahla, A.A., Tounsi, A., Alwabli, A.S., Tounsi, A. and Mahmoud, S. (2019), "Static analysis of laminated reinforced composite plates using a simple first-order shear deformation theory", *Comput. Concrete, Int. J.*, **24**(4), 369-378. https://doi.org/10.12989/cac.2019.24.4.369.

Draoui, A., Zidour, M., Tounsi, A. and Adim, B. (2019). "Static and dynamic behavior of nanotubes-reinforced sandwich plates using (FSDT)", *J. Nano Res.*, **57**, 117-135. https://doi.org/10.4028/www.scientific.net/JNanoR.57.117.

Ebrahimi, F. and Jafari, A. (2017), "Investigating vibration behavior of smart imperfect functionally graded beam subjected to magnetic-electric fields based on refined shear deformation theory", *Adv. Nano Res., Int. J.*, **5**(4), 281-301. https://doi.org/10.12989/anr.2017.5.4.281.

Ebrahimi, F. and Salari, E. (2019), "Effect of non-uniform temperature distributions on nonlocal vibration and buckling of inhomogeneous size-dependent beams", *Adv. Nano Res., Int. J.*, **6**(4), 377-397. https://doi.org/10.12989/anr.2018.6.4.377.

Ebrahimi, F., Karimiasl, M., Civalek, Ö. and Vinyas, M. (2019), "Surface effects on scale-dependent vibration behavior of flexoelectric sandwich nanobeams", *Adv. Nano Res., Int. J.*, **7**(2), 77-88. https://doi.org/10.12989/anr.2019.7.2.077.

Ebrahimi, F., Jafari, A. and Selvamani, R. (2020a), "Thermal buckling analysis of magneto-electro-elastic porous FG beam in thermal environment", *Adv. Nano Res., Int. J.*, **8**(1), 83-94. https://doi.org/10.12989/anr.2020.8.1.083.

Ebrahimi, F., Supeni, E.E.B., Habibi, M. and Safarpour, H. (2020b), "Frequency characteristics of a GPL-reinforced composite microdisk coupled with a piezoelectric layer", *Eur. Phys. J. Plus*, **135**(2), 144. https://doi.org/10.1140/epjp/s13360-020-00217-x.

Ehyaei, J. and Daman, M. (2017), "Free vibration analysis of double walled carbon nanotubes embedded in an elastic medium with initial imperfection", *Adv. Nano Res., Int. J.*, **5**(2), 179-192. https://doi.org/10.12989/anr.2017.5.2.179.

Emam, S. and Eltaher, M. (2016), "Buckling and postbuckling of composite beams in hygrothermal environments", *Compos. Struct.*, **152**, 665-675. https://doi.org/10.1016/j.compstruct.2016.05.029.

Emdadi, M., Mohammadimehr, M. and Navi, B.R. (2019), "Free vibration of an annular sandwich plate with CNTRC facesheets and FG porous cores using Ritz method", *Adv. Nano Res., Int. J.*, **7**(2), 109. https://doi.org/10.12989/anr.2019.7.2.109.

Eslami, M., Moghadam, H.A., Zayandehroodi, H. and Ghadimi, N. (2019), "A new formulation to reduce the number of variables and constraints to expedite SCUC in bulky power systems", *Proc. Nat. Aca. Sci. Ind. Sec. A Phys. Sci.*, **89**(2), 311-321. https://doi.org/10.1007/s40010-017-0475-1.

Firouz, M.H. and Ghadimi, N. (2016), "Concordant controllers based on FACTS and FPSS for solving wide-area in multi-machine power system", *J. Intell. Fuzzy Syst.*, **30**(2), 845-859. https://doi.org/10.3233/IFS-151807.

Ghabussi, A., Ashrafi, N., Shavalipour, A., Hosseinpour, A., Habibi, M., Moayedi, H., Babaei, B. and Safarpour, H. (2019), "Free vibration analysis of an electro-elastic GPLRC cylindrical shell surrounded by viscoelastic foundation using modified length-couple stress parameter", *Mech. Based Des. Struct. Mach.*, **2020**, 1-25. https://doi.org/10.1080/15397734.2019.1705166.

Ghabussi, A., Marnani, J.A. and Rohanimanesh, M.S. (2020), "Improving seismic performance of portal frame structures with steel curved dampers", *Structures*, **24**, 27-40. https://doi.org/10.1016/j.istruc.2019.12.025.

Ghannadpour, S. and Moradi, F. (2019), "Nonlocal nonlinear analysis of nano-graphene sheets under compression using semi-Galerkin technique", *Adv. Nano Res., Int. J.*, **7**(5), 311-324. https://doi.org/10.12989/anr.2019.7.5.311.

Gheydi, M., Nouri, A. and Ghadimi, N. (2016), "Planning in microgrids with conservation of voltage reduction", *IEEE Syst. J.*, **12**(3), 2782-2790. https://doi.org/10.1109/JSYST.2016.2633512.

Gollou, A.R. and Ghadimi, N. (2017), "A new feature selection and hybrid forecast engine for day-ahead price forecasting of electricity markets", *J. Intell. Fuzzy Syst.*, **32**(6), 4031-4045. https://doi.org/10.3233/JIFS-152073.

Habibi, M., Mohammadi, A., Safarpour, H., Shavalipour, A. and Ghadiri, M. (2019), "Wave propagation analysis of the laminated cylindrical nanoshell coupled with a piezoelectric actuator", *Mech. Based Des. Struct. Mach.*, **2019**, 1-19. https://doi.org/10.1080/15397734.2019.1697932.

Habibi, M., Safarpour, M. and Safarpour, H. (2020), "Vibrational characteristics of a FG-GPLRC viscoelastic thick annular plate using fourth-order Runge-Kutta and GDQ methods", *Mech. Based Des. Struct. Mach.*, **2020**, 1-22. https://doi.org/10.1080/15397734.2020.1779086.

Hamian, M., Darvishan, A., Hosseinzadeh, M., Lariche, M.J., Ghadimi, N. and Nouri, A. (2018), "A framework to expedite joint energy-reserve payment cost minimization using a custom-designed method based on mixed integer genetic algorithm", *Eng. Appl. Artif. Intell.*, **72**, 203-212. https://doi.org/10.1016/j.engappai.2018.03.022.

Hosseini Firouz, M. and Ghadimi, N. (2016), "Optimal preventive maintenance policy for electric power distribution systems based on the fuzzy AHP methods", *Complexity*, **21**(6), 70-88. https://doi.org/10.1002/cplx.21668.

Kaddari, M., Kaci, A., Bousahla, A.A., Tounsi, A., Bourada, F., Tounsi, A., Bedia, E. and Al-Osta, M.A. (2020), "A study on the structural behaviour of functionally graded porous plates on elastic foundation using a new quasi-3D model: Bending and free vibration analysis", *Comput. Concrete, Int. J.*, **25**(1), 37-57. https://doi.org/10.12989/cac.2020.25.1.037.

Karimiasl, M., Ebrahimi, F. and Akgöz, B. (2019), "Buckling and post-buckling responses of smart doubly curved composite shallow shells embedded in SMA fiber under hygro-thermal loading", *Compos. Struct.*, **223**, 110988. https://doi.org/10.1016/j.compstruct.2019.110988.

Khiloun, M., Bousahla, A.A., Kaci, A., Bessaim, A., Tounsi, A.

and Mahmoud, S. (2020), "Analytical modeling of bending and vibration of thick advanced composite plates using a four-variable quasi 3D HSDT", *Eng. Comput.*, **36**(3), 807-821. https://doi.org/10.1007/s00366-019-00732-1.

Khodaei, H., Hajiali, M., Darvishan, A., Sepehr, M. and Ghadimi, N. (2018), "Fuzzy-based heat and power hub models for cost-emission operation of an industrial consumer using compromise programming", *Appl. Therm. Eng.*, **137**, 395-405. https://doi.org/10.1016/j.applthermaleng.2018.04.008.

Kim, M., Park, Y.B., Okoli, O.I. and Zhang, C. (2009), "Processing, characterization, and modeling of carbon nanotube-reinforced multiscale composites", *Compos. Sci. Technol.*, **69**(3-4), 335-342. https://doi.org/10.1016/j.compscitech.2008.10.019.

Leng, H., Li, X., Zhu, J., Tang, H., Zhang, Z. and Ghadimi, N. (2018), "A new wind power prediction method based on ridgelet transforms, hybrid feature selection and closed-loop forecasting", *Adv. Eng. Inf.*, **36**, 20-30. https://doi.org/10.1016/j.aei.2018.02.006.

Liu, Y., Wang, W. and Ghadimi, N. (2017), "Electricity load forecasting by an improved forecast engine for building level consumers", *Energy*, **139**, 18-30. https://doi.org/10.1016/j.energy.2017.07.150.

Lori, E.S., Ebrahimi, F., Supeni, E.E.B., Habibi, M. and Safarpour, H. (2020), "The critical voltage of a GPL-reinforced composite microdisk covered with piezoelectric layer", *Eng. Comput.*, **2020**, 1-20. https://doi.org/10.1007/s00366-020-01004-z.

Maghamikia, S. and Jam, J. (2011), "Buckling analysis of circular and annular composite plates reinforced with carbon nanotubes using FEM", *J. Mech. Sci. Technol.*, **25**(11), 2805-2810. https://10.1007/s12206-011-0738-8.

Medani, M., Benahmed, A., Zidour, M., Heireche, H., Tounsi, A., Bousahla, A.A., Tounsi, A. and Mahmoud, S. (2019), "Static and dynamic behavior of (FG-CNT) reinforced porous sandwich plate using energy principle", *Steel Compos. Struct., Int. J.*, **32**(5), 595-610. https://doi.org/10.12989/scs.2019.32.5.595.

Menasria, A., Kaci, A., Bousahla, A.A., Bourada, F., Tounsi, A., Benrahou, K.H., Tounsi, A., Adda Bedia, E. and Mahmoud, S. (2020), "A four-unknown refined plate theory for dynamic analysis of FG-sandwich plates under various boundary conditions", *Steel Compos. Struct., Int. J.*, **36**(3), 355-367. https://doi.org/10.12989/scs.2020.36.3.355.

Mirzapour, F., Lakzaei, M., Varamini, G., Teimourian, M. and Ghadimi, N. (2019), "A new prediction model of battery and wind-solar output in hybrid power system", *J. Amb. Intell. Human. Comput.*, **10**(1), 77-87. https://doi.org/10.1007/s12652-017-0600-7.

Moayedi, H., Aliakbarlou, H., Jebeli, M., Noormohammadiarani, O., Habibi, M., Safarpour, H. and Foong, L. (2020a), "Thermal buckling responses of a graphene reinforced composite micropanel structure", *Int. J. Appl. Mech.*, **12**(1), 2050010. https://doi.org/10.1142/S1758825120500106.

Moayedi, H., Darabi, R., Ghabussi, A., Habibi, M. and Foong, L.K. (2020b), "Weld orientation effects on the formability of tailor welded thin steel sheets", *Thin-Wall. Struct.*, **149**, 106669. https://doi.org/10.1016/j.tws.2020.106669.

Oyarhossein, M.A., Alizadeh, A.A., Habibi, M., Makkiabadi, M., Daman, M., Safarpour, H. and Jung, D.W. (2020), "Dynamic response of the nonlocal strain-stress gradient in laminated polymer composites microtubes", *Sci. Rep.*, **10**(1), 1-19. https://doi.org/10.1038/s41598-020-61855-w.

Parand, A.A. and Alibeigloo, A. (2017), "Static and vibration analysis of sandwich cylindrical shell with functionally graded core and viscoelastic interface using DQM", *Compos. Part B Eng.*, **126**, 1-16. https://doi.org/10.1016/j.compositesb.2017.05.071.

Rabhi, M., Benrahou, K.H., Kaci, A., Houari, M.S.A., Bourada, F., Bousahla, A.A., Tounsi, A., Bedia, E.A., Mahmoud, S. and Tounsi, A. (2020), "A new innovative 3-unknowns HSDT for buckling and free vibration of exponentially graded sandwich plates resting on elastic foundations under various boundary conditions", *Geomech. Eng., Int. J.*, **22**(2), 119-132. https://doi.org/10.12989/gae.2020.22.2.119.

Rafiee, M., Yang, J. and Kitipornchai, S. (2013), "Large amplitude vibration of carbon nanotube reinforced functionally graded composite beams with piezoelectric layers", *Compos. Struct.*, **96**, 716-725. https://doi.org/10.1016/j.compstruct.2012.10.005.

Rafiee, M., Liu, X., He, X. and Kitipornchai, S. (2014), "Geometrically nonlinear free vibration of shear deformable piezoelectric carbon nanotube/fiber/polymer multiscale laminated composite plates", *J. Sound Vib.*, **333**(14), 3236-3251. https://doi.org/10.1016/j.jsv.2014.02.033.

Rahimi, A., Alibeigloo, A. and Safarpour, M. (2020), "Three-dimensional static and free vibration analysis of graphene platelet-reinforced porous composite cylindrical shell", *J. Vib. Control*, 1077546320902340. https://doi.org/10.1177/1077546320902340.

Rahmani, M.C., Kaci, A., Bousahla, A.A., Bourada, F., Tounsi, A., Bedia, E., Mahmoud, S., Benrahou, K.H. and Tounsi, A. (2020), "Influence of boundary conditions on the bending and free vibration behavior of FGM sandwich plates using a four-unknown refined integral plate theory", *Comput. Concrete., Int. J.*, **25**(3), 225-244. https://doi.org/10.12989/cac.2020.25.3.225.

Refrafi, S., Bousahla, A.A., Bouhadra, A., Menasria, A., Bourada, F., Tounsi, A., Bedia, E., Mahmoud, S., Benrahou, K.H. and Tounsi, A. (2020), "Effects of hygro-thermo-mechanical conditions on the buckling of FG sandwich plates resting on elastic foundations", *Comput. Concrete., Int. J.*, **25**(4), 311-325. https://doi.org/10.12989/cac.2020.25.4.311.

Safarpour, M., Rahimi, A. and Alibeigloo, A. (2019a), "Static and free vibration analysis of graphene platelets reinforced composite truncated conical shell, cylindrical shell, and annular plate using theory of elasticity and DQM", *Mech. Based Des. Struct. Mach.*, **2019**, 1-29. https://doi.org/10.1080/15397734.2019.1646137

Safarpour, M., Rahimi, A., Alibeigloo, A., Bisheh, H. and Forooghi, A. (2019b), "Parametric study of three-dimensional bending and frequency of FG-GPLRC porous circular and annular plates on different boundary conditions", *Mech. Based Des. Struct. Mach.*, **2019**, 1-31. https://doi.org/10.1080/15397734.2019.1701491.

Safarpour, M., Ghabussi, A., Ebrahimi, F., Habibi, M. and Safarpour, H. (2020), "Frequency characteristics of FG-GPLRC viscoelastic thick annular plate with the aid of GDQM", *Thin-Wall. Struct.*, **150**, 106683. https://doi.org/10.1016/j.tws.2020.106683.

Sahla, M., Saidi, H., Draiche, K., Bousahla, A.A., Bourada, F. and Tounsi, A. (2019), "Free vibration analysis of angle-ply laminated composite and soft core sandwich plates", *Steel Compos. Struct., Int. J.*, **33**(5), 663-679. https://doi.org/10.12989/scs.2019.33.5.663.

Salari, F.E.E. (2016), "Thermal loading effects on electro-mechanical vibration behavior of piezoelectrically actuated inhomogeneous size-dependent Timoshenko nanobeams", *Adv. Nano Res., Int. J.*, **4**(3), 197-228. https://doi.org/10.12989/anr.2016.4.3.197.

Salehipour, H., Shahgholian-Ghahfarokhi, D., Shahsavar, A., Civalek, O. and Edalati, M. (2020), "Static deflection and free vibration analysis of functionally graded and porous cylindrical micro/nano shells based on the three-dimensional elasticity and modified couple stress theories", *Mech. Based Des. Struct. Mach.*, **2020**, 1-22. https://doi.org/10.1080/15397734.2020.1775095.

Shaban, M. and Alibeigloo, A. (2020), "Global bending analysis of corrugated sandwich panels with integrated piezoelectric layers", *J. Sandw. Struct. Mater.*, **22**(4), 1055-1073. https://doi.org/10.1177/1099636218780172.

Shahsavari, D., Karami, B. and Janghorban, M. (2019), "Size-dependent vibration analysis of laminated composite plates", *Adv. Nano Res., Int. J.*, **7**(5), 337-349. https://doi.org/10.12989/anr.2019.7.5.337.

Shen, H.S. (2009), "A comparison of buckling and postbuckling behavior of FGM plates with piezoelectric fiber reinforced composite actuators", *Compos. Struct.*, **91**(3), 375-384. https://doi.org/10.1016/j.compstruct.2009.06.005.

Shokrgozar, A., Ghabussi, A., Ebrahimi, F., Habibi, M. and Safarpour, H. (2020), "Viscoelastic dynamics and static responses of a graphene nanoplatelets-reinforced composite cylindrical microshell", *Mech. Based Des. Struct. Mach.*, **2020**, 1-28. https://doi.org/10.1080/15397734.2020.1719509.

Shu, C. (2012), *Differential Quadrature and Its Application in Engineering*, Springer Science & Business Media, London, UK.

Shu, C. and Richards, B.E. (1992), "Application of generalized differential quadrature to solve two-dimensional incompressible Navier-Stokes equations", *Int. J. Num. Methods Fluids*, **15**(7), 791-798. https://doi.org/10.1002/fld.1650150704.

Tahouneh, V. and Eskandari-Jam, J. (2014), "A semi-analytical solution for 3-D dynamic analysis of thick continuously graded carbon nanotube-reinforced annular plates resting on a Two-parameter elastic foundation", *Mech. Adv. Compos. Struct.*, **1**(2), 113-130. https://doi.org/10.22075/macs.2014.286.

Tahouneh, V. and Yas, M. (2014), "Influence of equivalent continuum model based on the Eshelby-Mori-Tanaka scheme on the vibrational response of elastically supported thick continuously graded carbon nanotube-reinforced annular plates", *Polym. Compos.*, **35**(8), 1644-1661. https://doi.org/10.1002/pc.22818.

Thostenson, E., Li, W., Wang, D., Ren, Z. and Chou, T. (2002), "Carbon nanotube/carbon fiber hybrid multiscale composites", *J. Appl. Phys.*, **91**(9), 6034-6037. https://doi.org/10.1063/1.1466880.

Tounsi, A., Benguediab, S., Semmah, A. and Zidour, M. (2013), "Nonlocal effects on thermal buckling properties of double-walled carbon nanotubes", *Adv. Nano Res., Int. J.*, **1**(1), 1-11. https://doi.org/10.12989/anr.2013.1.1.001.

Tounsi, A., Al-Dulaijan, S., Al-Osta, M.A., Chikh, A., Al-Zahrani, M., Sharif, A. and Tounsi, A. (2020), "A four variable trigonometric integral plate theory for hygro-thermo-mechanical bending analysis of AFG ceramic-metal plates resting on a two-parameter elastic foundation", *Steel Compos. Struct., Int. J.*, **34**(4), 511-524. https://doi.org/10.12989/scs.2020.34.4.511.

Van Do, V.N. and Lee, C.H. (2020), "Static bending and free vibration analysis of multilayered composite cylindrical and spherical panels reinforced with graphene platelets by using isogeometric analysis method", *Eng. Struct.*, **215**, 110682. https://doi.org/10.1016/j.engstruct.2020.110682.

Wang, Q., Quek, S., Sun, C. and Liu, X. (2001), "Analysis of piezoelectric coupled circular plate", *Smart Mater. Struct.*, **10**(2), 229. https://doi.org/10.1088/0964-1726/10/2/308/meta

Wu, T., Wang, Y. and Liu, G. (2002), "Free vibration analysis of circular plates using generalized differential quadrature rule", *Comput. Methods Appl. Mech. Eng.*, **191**(46), 5365-5380. https://doi.org/10.1016/S0045-7825(02)00463-2.

Wu, H., Kitipornchai, S. and Yang, J. (2017), "Imperfection sensitivity of thermal post-buckling behaviour of functionally graded carbon nanotube-reinforced composite beams", *Appl. Math. Model.*, **42**, 735-752. https://doi.org/10.1016/j.apm.2016.10.045.

Wu, C.P., Chen, Y.H., Hong, Z.L. and Lin, C.H. (2018), "Nonlinear vibration analysis of an embedded multi-walled carbon nanotube", *Adv. Nano Res., Int. J.*, **6**(2), 163-182. https://doi.org/10.12989/anr.2018.6.2.163.

Yu, D. and Ghadimi, N. (2019), "Reliability constraint stochastic UC by considering the correlation of random variables with Copula theory", *IET Renew. Pow. Gen.*, **13**(14), 2587-2593. https://doi.org/10.1049/iet-rpg.2019.0485.

Zine, A., Bousahla, A.A., Bourada, F., Benrahou, K.H., Tounsi, A., Adda Bedia, E., Mahmoud, S. and Tounsi, A. (2020), "Bending analysis of functionally graded porous plates via a refined shear deformation theory", *Comput. Concrete, Int. J.*, **26**(1), 63-74. http://dx.doi.org/10.12989/cac.2020.26.1.063.

JL